Interplay between pinning energy and vortex interaction in $YBa_2Cu_3O_{7-\delta}$ with oriented twin boundaries in tilted magnetic fields: Bitter decoration and tilt-modulus measurements

J. A. Herbsommer, G. Nieva, and J. Luzuriaga
Centro Atómico Bariloche and Instituto Balseiro, CNEA and UNC, (8400) Bariloche, Argentina
(Received 25 March 1999; revised manuscript received 14 July 1999)

We have performed Bitter decoration and ac susceptibility measurements in single-crystal $YBa_2Cu_3O_{7-\delta}$ with oriented twin boundaries. The twin boundaries (TB's) pin vortices over approximately 65% of the sample. The pinned areas are unevenly distributed and some relatively large TB-free regions are present. The Bitter decorations were performed in a 52 Oe dc magnetic field rotated off the *c* axis so that the plane defined by the field direction and the *c* axis is perpendicular to the TB's. Several decorations were performed in the same sample. Additional dynamical information was obtained from ac susceptibility measurements. Results show that for small tilts the vortices remain locked to the *c*-axis direction, for angles greater than 12° they form a staircase pattern, and in this case pinning by the twin boundaries remains effective up to 75°. We observe vortex chains in twin-free zones of the sample for tilted fields at 65° and 40°. Due to our particular experimental arrangement, in the twinned regions the interplay of the potentials giving rise to the chains and the pinning potential produces a structure with a disordered square symmetry. The data allow us to estimate the dominant energy of the vortex system for some inclinations of the applied magnetic field.

I. INTRODUCTION

The vortex structures found in high-T_c superconductors show a rich variety of forms, connected to the various thermodynamic phases of the vortex phase diagram. The interplay between temperature, pinning energy, and the vortex lattice elastic constants is responsible for this complex behavior.[1] The anisotropy of the materials adds another dimension, since the vortex lattice is affected by the orientation of the field with respect to the crystal axes.[2,3] There has been extensive research into this problem, both for its fundamental and applied interest. Recently the interaction between elastic manifolds and disordered pinning potentials and their dynamical properties has also become a subject of theoretical[4] and experimental work.[5,6]

In this context, we present results of Bitter decorations and susceptibility measurements performed on the same sample, allowing a simultaneous measurement of vortex lattice dynamics and structure in a high-T_c material. We have chosen $YBa_2Cu_3O_{7-\delta}$ (YBCO) for our study. The main reason is that in this compound there are twin boundaries[11] (TB's) which form extended, planarly correlated pinning centers for the vortices. A second reason is the fact that several previous decoration studies make this a well-characterized material.[7–10]

In our particular case, we study a sample with TB's oriented in only one direction. When tilting an external magnetic field with rotation axis in the ab planes and perpendicular to the twin boundary planes there is a systematic change in the vortex-vortex interaction (because of the anisotropy) and in the effect of pinning by twin boundaries. Also, by orienting the ac field of the susceptibility measurements along the ab planes and parallel to the twin boundaries, a tilt force acts on the vortices parallel to the TB, allowing the study of dynamical properties in this direction.

The pinning by correlated defects is expected to be maximum when both the defect and the applied field are aligned, and in this case, over a small angular range, in the *lock-in* regime the vortices will follow the defect, and not the direction of the field. For larger angles, an *accommodation* regime is expected, where the vortices are partially aligned with the defects, and for larger misalignment of field and defect a free vortex state is found.[1,12–16] Our results, combining dynamical and structural evidence, show the *lock-in* regime clearly, but also indicate that in some parts of the sample between TB's, part of the vortices are aligned with the field. In the transition from the *accommodation* to the free vortex regime, there seems to be a marked difference in dynamical properties, which is not abrupt in the static structure of the vortex lattice.

The interplay between the material anisotropy which tends to align the vortices along chains in tilted fields[17,18] and the pinning of the twin boundaries, which run at right angles to the chains in our configuration, gives us the possibility of estimating the dominant energy of the problem at different angles of the field.

II. EXPERIMENTAL DETAILS

The YBCO crystal comes from a batch prepared using a flux-growth technique as described in Ref. 19, and was fully oxygenated with a T_c value of 92.5 K and a zero-field transition width $\Delta T = 0.6$ K (taken from the width at half maximum of the peak in the ac susceptibility measurement). Observation by polarized light showed a single orientation for the twin boundaries. This was further confirmed by the decoration experiments which show no evidence of TB's in other directions. The crystal has the shape of a slab with approximate dimensions $(1 \times 2 \times 0.03)$ mm^3.

Decorations by the Bitter technique[20] were performed at 4.2 K using a field cooling (FC) procedure for different angles of the applied magnetic field, keeping the modulus fixed at 52 Oe. The magnetic field was rotated using an ad-

 ©2000 The American Physical Society

ditional coil perpendicular to the first, in a direction such that the plane defined by the field and the *c* axis is perpendicular to the twin boundary planes. The sample was warmed up and scanning electron microscope (SEM) images were obtained. The resolution of the images was 330 pixels/μm^2. A cleaning procedure with isopropyl alcohol under ultrasound agitation was performed before each decoration experiment in order to remove thoroughly the iron particles of previous experiments. The sample was glued with silver paint to the same sample holder throughout the experiments and care was taken to keep the same relative orientation between the rotation plane of magnetic field and the twin boundaries.

By analyzing the decorations over the whole area of the sample, it can be seen, when the applied field is parallel to the *c* axis, that around 65% of the vortices are locked to the twin boundaries, with TB-free regions scattered in irregular bands in between. While a few twin-boundary-free bands were as much as 100 vortex lattice parameters $a_0 \simeq \sqrt{\Phi_0/H}$ $\simeq 0.62$ μm broad, most were narrower, typically $(10-15)a_0$.

Information about lattice dynamics was obtained by means of ac susceptibility measurements on the same sample. The ac field h_{ac} was applied in the ab plane, perpendicular to the dc field H and parallel to the TB's. In this configuration, the force on the vortices will tend to tilt them parallel to the TB direction. These measurements were carried out by means of mutual inductance technique and the excitation and detection was made by means of a two-phase lock-in amplifier (PAR 5302). The proper phase of the lock-in amplifier was set by measuring the sharp superconducting transition of an indium sample. All the susceptibility measurements reported here have been taken in FC experiments with the applied field of $H=52$ Oe at different angles.

III. RESULTS AND DISCUSSION

A. Bitter decoration

The magnetic decorations were performed on the ab plane and in all the images of the present paper, the twin boundaries of the crystal are oriented vertically, (y coordinate), and the projection of the tilted field is in the horizontal (x coordinate) direction.

1. Field in the c-axis direction

Figure 1 shows the typical decoration pattern obtained in the TB-free regions of the sample corresponding to a FC experiment with the field in the *c*-axis direction.

The image shows a very ordered lattice, with a systematic deformation due to the anisotropy of the penetration length λ between the *a* and *b* axis.[21] This is evident in the Fourier transform (FT) of the inset in Fig. 1 which shows the average over 12 different areas of the sample in reciprocal space. It is clear that a particular orientation dominates sufficiently that an hexagonal elliptical pattern is obtained even after averaging. An ellipse was fitted to the transform. The best fit gives an eccentricity of 1.2 and a major axis oriented 49° away from the twin direction. These values agree with those reported by Dolan *et al.*[21] The orientation of the vortex lattice in all TB-free regions has always a compact vortex plane aligned in the direction of the twin boundaries.

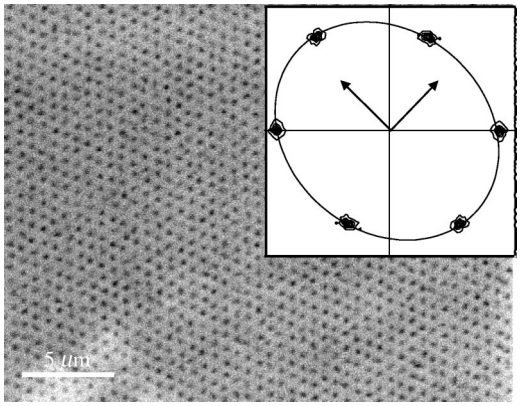

FIG. 1. Decoration with the field parallel to the *c* axis in a twin-free region of the sample. Inset: Fourier transform averaging over 12 similar images. The arrows indicate the orientation of the ab crystallographic axes. All images are presented so that the twin boundary planes are shown in a vertical direction; notice that in this picture a compact vortex plane can be seen in the vertical direction.

This orientation was maintained over distances as large as 100 times a_0, indicating that the influence of the TB's extends over at least this distance. One possible explanation is that the twin boundary acts as a nucleation center for the vortex crystal, which then grows with the observed orientation. The point disorder does not seem to be strong enough to decorrelate the vortex lattice over these distances. It is interesting to remark that the data of Dolan *et al.*[21] show the same relative orientation between the twin boundaries and the vortex lattice. According to Campbell *et al.*[2] in an anisotropic superconductor with the field perpendicular to both anisotropy axes, no orientation of the vortex lattice distortion is favored, so the coincidence must be due to the orientation produced by the TB's in both samples.

The induction field *B*, obtained by averaging the number of vortices over 12 images of $\sim$1300 vortices each, is 45.5 Oe with a dispersion of 0.5 Oe, which means that there is a flux expulsion of 6.5 Oe, corresponding to the average magnetization of the sample.[22]

In Fig. 2 we show a typical image obtained from the same

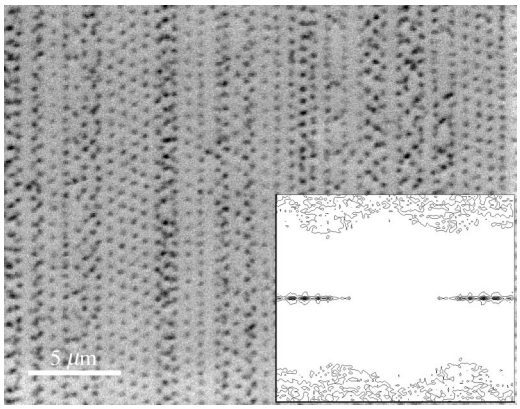

FIG. 2. Decoration with field parallel to the *c* axis in a twinned region of the sample. The twin boundaries are clearly evident as vertical columns where the vortex density is increased. Inset: Fourier transform over 12 similar areas of the sample.

decoration experiment but in a twinned region of the sample. Each TB acts as a potential well in the form of a channel pinning vortices (visible as vortex ''columns'' in the vertical direction in the figure). The lattice parameter along each channel is different and characteristic of a given TB so that the hexagonal symmetry is lost. Also, since the x coordinate of the TB's is random the structure is disordered in the x direction so there is no long-range order either along the y or x directions, but there remains a strong orientational order along y. To complement the information of the direct image we use the FT in the inset of the same figure corresponding to a set of 12 images similar to the one shown. The central horizontal lines of the pattern correspond to the family of vortex planes pinned by the TB's. The extension of these lines is a measure of the dispersion in the distance between vortex columns. The bands in the top and bottom represent the decorrelation between the vortices in the different vortex columns. As a test of these ideas we performed simulations starting with ordered lattices and introducing successive disorder, first in the correlation between columns, then in the column lattice parameter, and last in the column position along the x axis. We studied the resultant FT, finding that it evolves with the successive decorrelations towards the same type of image seen in the FT of the decorations.

Averaging over ten pictures of ~ 1300 vortices each, we find an induction field B of 45 Oe with a dispersion of 1 Oe. It is remarkable that B has the same average value in both the twinned and the TB-free region. Inspection of the vortices at the frontier shows that the deformations of the vortex lattice near a TB propagate one or two lattice parameters into the TB-free region so that the total magnetic flux is restored over this distance. For the tilted magnetic fields reported in the following sections the average number of vortices also remains the same in zones of the sample showing effective vortex pinning by TB's or regions with no pinning by twin boundaries.

The pinning energy dominates over the interaction energy here, as can be inferred from the fact that the hexagonal lattice is completely lost. Because neighboring TB planes have different vortex densities, in general the (vertical) columns of vortices seen in the decorations have incommensurate lattice parameters. However, there still remains a repulsion between vortex lines seen over short distances where vortices in one column align with gaps in a neighboring one. Because of the incommensurability, however, this does not persist over long distances.

Using the expressions of the repulsive interaction between vortices of the London theory the interaction elastic energy stored in the vortex lattice can be calculated from the coordinates of the vortex images. In the twinned regions we obtain an average energy 25% higher and with more dispersion over different parts of the sample than in TB-free zones. The balance of the internal energy is supplied by the pinning potential.

We evaluated the elastic energy that results when displacing the coordinates of the positions of a column of vortices along the y axis, leaving the coordinates of neighboring vortices unchanged. We find that the original position minimizes the elastic energy. Displacements smaller than the mean vortex distance along the column raise the energy, and when the displacement is close to the mean vortex distance there is a new but much shallower minimum, implying an imperfect periodicity of the interaction potential in the column's direction.

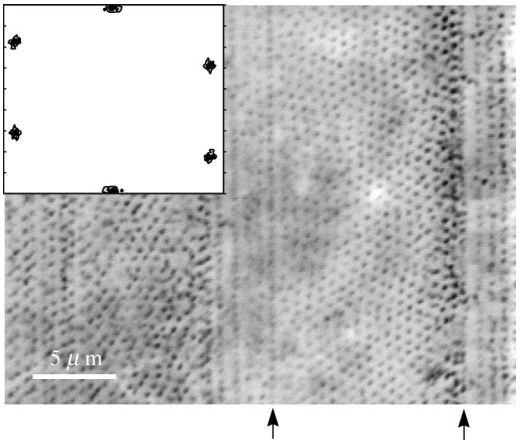

FIG. 3. Image in a twinned region of the sample with the field tilted 8° from the c axis. There is a small twin-free region between the arrows; notice the piling up of vortices at the right and stretching at the left boundaries of this area. Inset: FT of a twin-free region of the sample for the same field tilt (direct image is not shown).

Because the vortices are relatively rigid rods aligned by the TB's, it may be possible to treat two neighboring vortex lines as interacting one-dimensional incommensurate elastic manifolds, such as in the Frenkel-Kontorova model.[23–25] The model has solutions with compression and expansion regions, ordered in the simplest cases,[24] and disordered otherwise.[25] We have observed compression and expansion regions along the vortex columns, with no long-range order. This could be an effect of the residual disorder on the twin pinning potential, so a comparison with the models is difficult, although it could be an interesting problem for future study. For other systems in the literature[26] buckling of linear vortex structures has been reported, and in fact we have seen buckling in some of the vortex columns pinned to the TB's in the decorations at $\theta = 0°$. This complicates the situation and indicates that the direction perpendicular to the columns cannot be completely ignored.

2. Field tilted 8° from the c axis

Figure 3 shows a decoration with the applied field tilted 8° from the c axis, in a partially twinned region of the sample. This type of pattern is not exceptional but is observed in several places.

An almost hexagonal lattice is seen in a region between the TB's, extending around 18 lattice parameters, from the left arrow to the right one in Fig. 3. There are two important differences with respect to equivalent decorations with the field in the c axis. The first is that the lattice is deformed: the vortices pile up near the TB plane at the right hand side, and are stretched close to the TB plane to the left of the image.

This can be seen in Fig. 4 which shows the average density of vortices as a function of the distance along the x direction between the arrows in the previous figure. This profile can be understood if we consider that vortices are locked inside the TB's and follow the applied field between TB's. The field is tilted towards the right side of the figure, which would provide the deformation observed. The sample

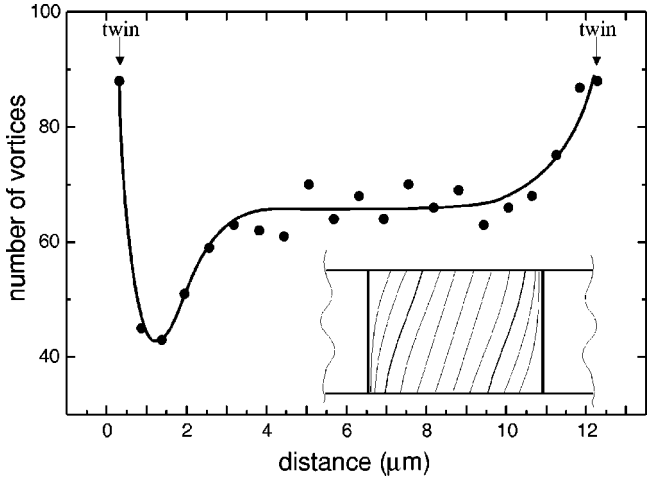

FIG. 4. Number of vortices as a function of the displacement along x for the region between the arrows in the previous figure. Inset: schematic side view of the displacement of vortices in a twin-free region between two twin boundaries, when there is vortex locking at the twin boundaries.

is 30 μm thick, so that a region of $\sim 30 \sin(8°)$ μm $\simeq 4$ μm will be deformed as sketched in the inset of Fig. 4 in agreement with the width of the deformed regions.

The second important difference is the disorder of the lattice in the TB-free regions. Although the hexagonal symmetry is preserved, there is more disorder than with the field parallel to the c axis. If the ordered lattice is produced by nucleation and growth from the twin boundary plane, the disorder observed in the tilted field can be explained by taking into account the fact that there is an additional deformation at the twin boundary. The deformation, which arises from the piling up (or stretching) of the vortices, propagates into the nucleating crystal. We also observe that in the larger twin-free regions of the sample, the hexagonal lattice is more ordered, but now it is no longer a single crystal and we have found some grain boundaries. In at least one region more than $50a_0$ away from a TB, we found that the hexagonal lattice is rotated. The new orientation is such that a compact vortex line is along the x direction. The corresponding Fourier transform is shown in the inset of Fig. 3, and the two spots aligned vertically indicate a compact horizontal plane, in contrast to the spots aligned horizontally seen in the inset of Fig. 1. The ellipse parameters are now 1.16 for the eccentricity and 52° for the angle of the major axis.

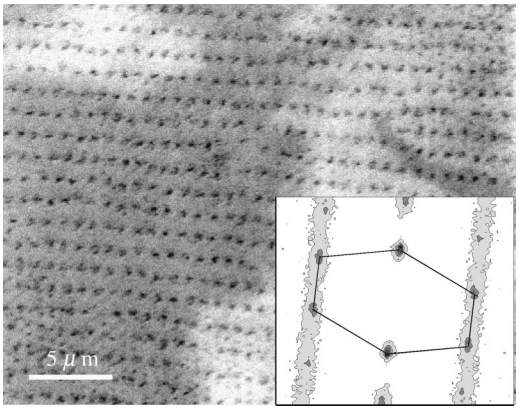

FIG. 5. Image in a twin-free region of the sample with the field tilted 65° from the c axis. The vortex chains can be clearly seen, running in a horizontal direction. As a consequence of a small misalignment of the field they are not exactly perpendicular to the (vertical) twin boundary direction. Inset: FT averaging over 12 similar images. Notice the hexagonal symmetry with bands indicative of disorder.

The fact that the field is tilted in this case introduces a further complication. Campbell *et al.*[2] calculate that for a tilted field in an anisotropic superconductor, there is both a vortex lattice distortion and a preferred lattice orientation, with a compact plane perpendicular to the rotation axis (i.e., it should be horizontal in our images). The distortion calculated from their theory in YBCO at 8° is less than 1%, much less than the almost 20% distortion from the ab anisotropy. Unfortunately the theory only treats anisotropy in two axes, and does not include the effects of the vortex chains,[27] so the degree of orientation due to the tilt at 8° remains an open question.

3. Field tilted 65° from the c axis

In Fig. 5 we show an image of the pattern obtained in a decoration with the applied field tilted 65° away from the c axis, in a TB-free region of the sample. We have also performed decorations with the field tilted 40° from the c axis and find qualitatively very similar results to those described below for 65°. In particular, we find that the deformation (piling up and stretching) of the vortex lattice images seen at 8° tilt at the frontier of the TB-free and twinned regions disappears at higher tilt.

As was seen previously in BSCCO (Ref. 17) and YBCO (Ref. 18) the vortices arrange in chains along the direction of the rotated field. Solution of the anisotropic London equations[27] in the limit $H \rightarrow H_{c1}$ reveals an attractive vortex-vortex interaction with potential wells in the direction along the chains. The vortices in fields just above H_{c1} will sit in these wells forming the chains. The spacing between the chains is set by the requirement that the average vortex density be correct.

The inset of the same figure shows the FT averaged over 12 TB-free areas. We can see six peaks indicating an hexagonal symmetry although (in contrast with the experiment with the field in the c axis) we can observe the presence of vertical bands and the peaks in the bands are less intense than the central ones, indicating a developing decorrelation between the chains. In agreement with Gammel *et al.*[18] we find that in this range of fields and angles the intrachain distance is almost field independent (0.97 μm here) and that the interchain distance (1.35 μm) accommodates to conserve the magnetic flux. Therefore increasing angles implies similar intrachain distances but increasing interchain distance, which means less interaction among the chains and favors decorrelation. However, a weak interaction between chains remains, as can be inferred from the hexagonal symmetry observed. It is energetically favorable to place a vortex in one chain facing a gap in the neighboring chain due to vortex-vortex repulsion, ordering the chains in the hexagonal pattern evident in the FT. Because of the weakness of the interaction, there is a considerable disorder, possibly due to point pinning, producing the bands seen in the FT. The existence of relatively narrow peaks indicates that the distance

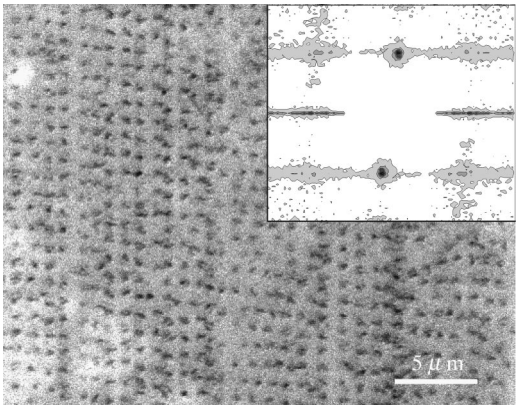

FIG. 6. Image in a twinned region of the sample with the field tilted 65° from the *c* axis. The vortex chains can still be seen in the horizontal direction but they are deformed by the twin boundaries, whose vertical orientation is also evident. Inset: FT averaging over 12 similar images. Notice the bands and the tendency to square symmetry.

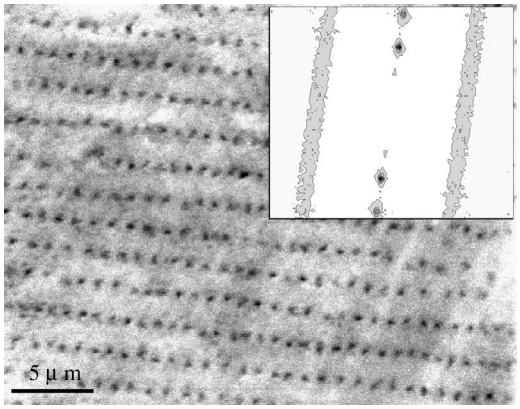

FIG. 7. Image in a twin-free region of the sample with the field at 75° from the *c* axis. Inset: FT averaging over 12 similar images showing decorrelated narrow bands, which indicate a well-defined interchain and intrachain spacing, but decorrelation between the chains.

between the chains and the intrachain lattice parameter are not affected too much by the point disorder.

In the twinned region the images are qualitatively different as shown in Fig. 6. The characteristic alignment of the vortices in the TB's is seen along *y* in ''columns'' but in addition vortex chains are visible, running almost parallel to the *x* axis. Comparing this pattern with the images of Fig. 2 we can see that the relative density of vortices in the twin boundaries is higher in Fig. 2. Therefore the effectiveness of the TB's to pin the vortices is diminishing. In fact, in Fig. 6 we can observe that there are some columns that have a ''lattice parameter'' shorter than the interchain distance but there are others that only correlate the vortices along the *y*-axis direction, while the interchain distance remains the same. This can be confirmed by analyzing the FT in the inset of the same figure. There are sharp peaks which define the reciprocal vector perpendicular to the family of planes formed by the chains and the horizontally stretched peaks correspond to the family of planes defined by the twin boundaries. The stretched characteristic is due to the fact that there is no periodicity of the *x* coordinate of the TB's and therefore there is a dispersion in the reciprocal vector corresponding to these planes. Here, we see a competition between two potentials tending to align the vortices in mutually perpendicular directions. The interactions forming the chains favors a constant lattice parameter along *x*,[27,18] but the presence of the channel-shaped potentials of the TB's that have random *x* coordinates changes these coordinates in order to gain pinning energy. By means of these two perpendicular potentials and despite the nonperiodicity introduced by the TB's the symmetry of the lattice is changing from hexagonal to rectangular. This implies that both potentials are important in determining the structure and there is no dominant energy in this case.

4. Field tilted 75° from the c axis

In Fig. 7 we show a typical image of the vortex structure in a TB-free zone of the sample corresponding to a field tilted 75° away from the *c* axis.

We can clearly see the chains and in agreement with the observations of Gammel *et al.*[18] the intrachain distance is similar (1.06 μm here, compared to 0.97 μm at 65°) and the distance between chains is different (2 μm compared to 1.35 μm at 65°).

The interaction between the chains is reduced because they are further apart producing important changes in the ordering of the lattice. Looking at the FT in the inset of Fig. 7 we can appreciate the vertical bands indicating almost complete decorrelation between the chains. It therefore seems that the dominant energy scale at this angle is the ''chain potential'' with a comparable but possibly smaller contribution due to the ''pinning potential'' and an almost negligible interaction between neighboring chains.

Figure 8 is a typical image of the same decoration experiment but in a twinned area of the sample. The tendency seen previously is confirmed and the effectiveness of the twin boundaries continues to decrease with increasing angle. From this picture we can see that most of the twin bound-

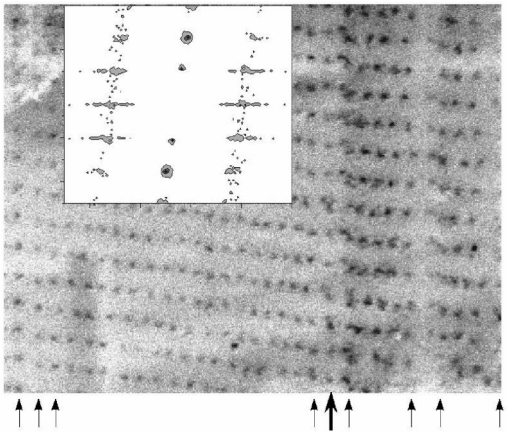

FIG. 8. Image in a twinned region of the sample with the field at 75° from the *c* axis. The pinning effect of the twin boundaries is visible in the vertical line marked with arrows. Inset: FT showing an almost square lattice, produced by the vertical correlation at a few points and the horizontal correlation produced by the chain potential.

aries (marked with arrows) are only effective in correlating the vortices along the *y*-axis direction but they are not capable of enhancing the vortex density along them.

Few columns with increased vortex density are seen, and in some cases the vortices are displaced a little in the *x* direction. The thick arrow marks a TB in Fig. 8 in which we can appreciate that the vortices are not aligned with the TB but are forming kinks in the vortex column pinned to the twin boundary. In this way they gain some pinning energy from the TB and some interaction energy by aligning with the chain despite of repulsion energy they lose by being close together in pairs. The existence of kinks where the chains intersect the TB's argues for a rough equivalence between chain and TB pinning potentials.

The remaining influence of some of the TB's produces a correlation along the *y* axis. In fact a tendency to place vortices in neighboring chains in front of each other is observed, and this produces the rectangular correlation seen in the FT of Fig. 8. The interaction between chains is not so important since they are farther apart. Therefore, the chains can optimize their pinning energy by having a vortex inside one of the few remaining strong pinning twin boundaries disregarding interchain repulsion. In the limit where only a single TB is effective and one vortex in each chain becomes pinned to it, perfect correlation in the *y* direction would result. Correlation would also propagate along *x*, because the spacing along the chains is set by the constant chain potential. However, when several TB's are present at random intervals and with possible random point pinning the imperfect lattice observed is obtained instead.

In the inset of Fig. 8 we show the FT corresponding to 12 different pictures taken in twinned regions from the last experiment. The characteristics described above are confirmed in the Fourier transform: this corresponds to an almost rectangular vortex structure. The slight horizontal stretching of the peaks is due to the nonperiodic position of the TB's but it is important to remark that this feature is much less pronounced than for smaller tilt in *H*.

In FC decoration experiments, although they are performed close to 4.2 K, the lattice observed has solidified at a higher temperature as also observed in Refs. 18, 28, and 29. This is inferred from the fact that in all our magnetic decorations the average vortex density at the crystal surface, measured from the decoration pattern, was close to the typical equilibrium magnetization[22] seen at higher temperatures. This indicates a freezing of the vortices, due to the slow vortex creep below the vortex liquid-solid transition. For the same reason, it is meaningful to compare the ac susceptibility measurements at the shielding onset T^* with the decorations.

Thus, we infer that our decorations at 4.2 K have information about the phases formed at the transition from the liquid to the solid state. For values of $\theta \sim 0$ and 8° the solid shows only orientational order and there is evidence for a *lock-in* phase. Grigera *et al.*[30] have shown by a scaling analysis that for small tilts the transition is to a Bose glass, while for larger angles no scaling can be shown and there appears to be a change in the order of the transition. For intermediate angles $\theta = 40°$ and $\theta = 65°$ our decorations show that the lock-in phase has been lost. Because the experiments of Grigera *et al.*[30] are at much higher fields, we must be cautious to make conclusions, but there is a rough correspondence between the scaling region[30] and the lock-in region.

Other decoration experiments on YBCO (Ref. 7) find that the effectiveness of the pinning by the TB's disappears for angles greater than $\sim 45°$ in contrast to what we see above. We do not know the reason for the discrepancy, but it could be due either to a difference in the quality of the different samples or to the fact that the crystals of Grigorieva *et al.*[7] have TB's in perpendicular directions which may decrease the overall pinning effectiveness in tilted fields. The effectiveness of the pinning at high angles is also surprising if one considers some theoretical estimates.[13] In this last reference, the pinning potential was estimated from decorations at 4.2 K and the elastic energy of the lattice was estimated at that temperature. However, the lattice is frozen in well above the decoration temperature, and this was not taken into account in the theory, so that there is a need for better estimates.

B. Susceptibility

In this section we show the results of ac susceptibility measurements we performed in the same sample in order to correlate static (magnetic decorations) and dynamic (ac susceptibility) properties of the vortex lattice. We measured the transverse ac susceptibility $\chi_\perp$ in the linear regime. The real component $\chi'_\perp$ is related to the shielding capability of the currents while $\chi''_\perp$, the imaginary part, is related to the dissipation. In the inset of Fig. 10, below, we show the configuration of the magnetic fields applied: the dc magnetic field $H = 52$ Oe is tilted in a plane perpendicular to the oriented twin boundaries and a small ac field h_{ac} is applied in the ab planes parallel to the TB's. In this way the ac currents induced in the sample are forced to flow in two directions, on the ab planes and across them. The Lorentz forces generated by the shielding currents exert a tilting stress on the vortex lattice in a plane parallel to the twin boundaries.

The ac susceptibility data were taken with a frequency $f = 2318$ Hz and with the ac field amplitude $h_{AC} = 90$ mOe. We checked that the response was within the linear regime over the whole range of dc fields and temperatures reported. We also confirmed that all our measurements are consistent with a Campbell[31,32] regime. In fact, from frequency dependence measurements, analysis of $\chi'_\perp$ vs $\chi''_\perp$ curves, and ac penetration length studies we conclude that in our experiment the tilting stress is small enough to only move the vortices in the bottom of their pinning potential wells. More details of this analysis will be reported in a future publication.

In Fig. 9 we show the results of the real part of the ac susceptibility, $\chi'_\perp$ (upper panel), and imaginary part $\chi''_\perp$ as a function of temperature for four selected angles.

From these curves we have determined the temperature T^* at which a fixed value of the screening $\chi'_\perp = -0.45$ is reached, as a function of the angle of the magnetic field. Figure 10 shows the angular variation of T^*. As the vortices are oriented in a different direction with respect to the crystal axes it is expected that the response will evolve following the characteristic anisotropy curve, as found, e.g., in Ref. 14. However, the observed T^* does not follow the behavior typical of the crystal anisotropy, which should have a shallow minimum around the *c* axis, and we attribute this behavior to

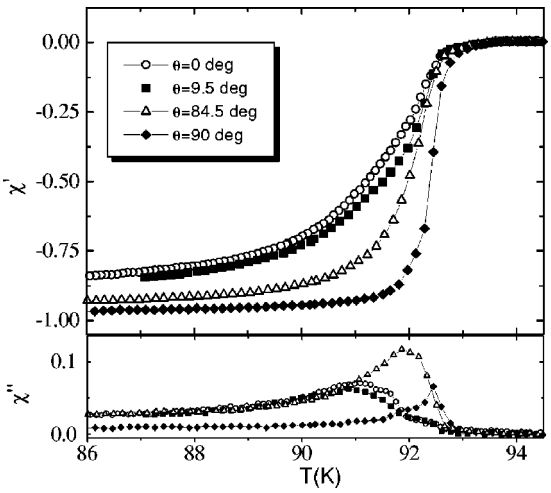

FIG. 9. Real part of the susceptibility $\chi_\perp'$ (upper panel) and imaginary part $\chi_\perp''$ (lower panel) as a function of temperature for different values of the angle between the dc magnetic field and the *c* axis of the crystal.

the effect of pinning by the TB's. With $\theta=0$ $(H\|c)$ there is a dip in the curve showing that the temperature must be lower to reach a given screening, indicating a ''softer'' lattice. As the field is tilted, the lattice seems to increase its stiffness until around $\theta=12°$ where again T^* decreases for increasing angles. A minimum in T^* is observed again for $\theta\simeq 70°$ and then there is an abrupt increase. The increase is again much higher than expected from the anisotropy of the material, and could be due to pinning in by the Cu-O planes.

These features of the susceptibility can be related to the features observed in decoration experiments. Decorations have been performed at the angles indicated by arrows in Fig. 10.

At $\theta=0$ the lattice outside the zone with TB's is ordered, and seems to be weaker with respect to the shear strain produced by h_{ac} than at $\theta=8°$. This can be understood if we recall that near twin boundaries, we observe a deformation which effectively couples the vortices between the TB's to those inside. This enhances the shear modulus of the structure, increasing the shielding capability.

Transport measurements by Kwok *et al.*[33] in tilted fields and similar force configuration on the vortices have been interpreted in this way, although the angles over which enhancement is observed are smaller. However, susceptibility measurements at higher fields in our samples, show that this angle decreases with field.

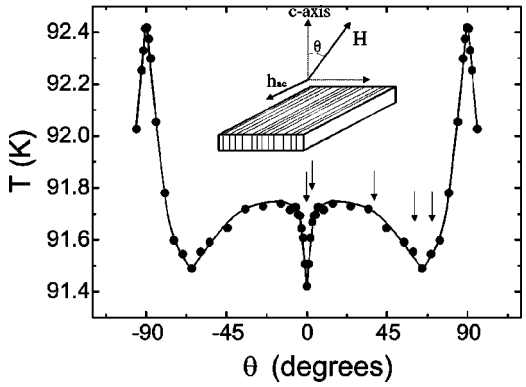

FIG. 10. Temperature where the shielding reaches 45% of total screening, as a function of angle. Inset: configuration of the ac and dc fields, with respect to the twin boundaries and axes of the sample.

We observe a maximum in T^* is detected in $\theta=12°$ and for angles greater than this value a decrease in the screening capability of the system as is usual in the angular dependence corresponding to susceptibility measurements of samples with correlated defects.[14] This decrease of the effectiveness of the pinning with angle is usually interpreted as due to a loss of pinning efficiency in the *accommodation* regime[1,12–16] since the vortices are partially pinned to the correlated defects in a staircase pattern and the pinned fraction decreases with angle. Although decorations only show the vortices coming out of the upper ab plane of the crystal, they are consistent with a staircase pattern when $\theta=40°$ and $\theta=65°$. There is no deformation of the vortex lattice in the frontiers between the TB and TB-free regions, indicating that the lock-in effect is lost in this angular range. We continue detecting ''free'' and pinned vortices in the images with smaller vortex density enhancement in the TB's, indicating that the pinning at the TB's has reached a small value.

Looking at images taken at angles greater and smaller than 70°, the change in structure in the decorations is relatively subtle. However, the dynamics of the FLL suffers an abrupt change at $\theta\sim 70°$. We can understand this contrast if we imagine a change in the FLL that modifies the dynamics and consequently the results of ac susceptibility but does not greatly affect the pattern of a decoration in the surface sample. One possibility is that the free segments of the staircase vortices lock in the Cu-O planes. In this situation, with segments pinned to the TB's and segments locked in the Cu-O planes, the restriction for the vortices to tilt is more important than in the previous arrangement. This change seriously affects the dynamics but probably is undetectable for the decoration experiment.

IV. CONCLUSIONS

The changes in the pinning of the twin boundaries as the field is rotated have been investigated by means of Bitter magnetic decoration and ac susceptibility. We have found evidence that for small tilts away from the *c* axis, the vortices inside the TB's remain locked to the *c*-axis direction, while those outside the TB follow the direction of the magnetic field. This induces a deformation of the FLL that enhances the shear constant of the lattice. It is confirmed by an abrupt increase in the screening capability in the ac susceptibility for angles up to 12°. For angles greater than 12° we find our results consistent with an image in which the vortices arrange in a staircase pattern. In this range we lose the deformations in the frontiers between twinned and twin-free areas and we see the usual decrease of the screening with angle due to the weakening of the correlated pinning potential. In this range (12°–70°) there is a competition between the TB pinning potential and the chain potential which are perpendicular to each other. The deformations of the flux line lattice produced by the TB and the chain potential can change the symmetry from hexagonal to almost square. In $\theta\sim 70°$ we detect through the ac susceptibility an abrupt increase in the screening capability which we interpret as a lock-in of the

free segments of the staircase vortices into the Cu-O planes. This change is not detected in the magnetic decoration.

In addition to the previous results we found that the twin boundaries probably act as a centers of nucleation during the growth of the vortex lattice. In the *c*-axis decoration we found a preferred orientation of the lattice in the twin-free region which is the one that has a compact plane parallel to the twin boundary. For the decoration of 8° away from the *c* axis the deformation in the boundary between twinned and twin-free zones propagates into the twin-free region at least $50a_0$ away from the TB that acts as a seed.

We have demonstrated that the study of the structures that result from the tilting of the field in a geometry as described above is an excellent way to understand the interplay and competition of two correlated potentials at right angles from each other. Tilting the field we can modify the relative importance of the energy of interaction and the pinning energy and in this way a fine-tuning of these energies scales is possible. Moreover, we have showed that the combination of two very different experimental techniques can be a powerful way of comparing the dynamics and static characteristics of the vortex structure.

ACKNOWLEDGMENTS

We thank F. de la Cruz for fruitful discussions and H. Pastoriza for a critical reading of the manuscript. This work was partially supported by the Consejo Nacional de Investigaciones Científicas y Técnicas (CONICET–Grant No. PIP 96/4207) and the Agencia Nacional de Promoción Científica y Tecnológica (Grant No. 03-00061-01120). J.A.H. acknowledges support by CONICET. G.N. belongs to CONICET's regular staff.

[1] G. Blatter, M. V. Feigel'man, V. B. Geshkenbein, A. I. Larkin, and V. M. Vinokur, Rev. Mod. Phys. **66**, 1125 (1994).
[2] L. J. Campbell, M. M. Doria, and V. G. Kogan, Phys. Rev. B **38**, 2439 (1988).
[3] V. G. Kogan and L. J. Campbell, Phys. Rev. Lett. **62**, 1552 (1989).
[4] P. Le Doussal and T. Giamarchi, Phys. Rev. B **57**, 11 356 (1998).
[5] F. Pardo, F. de la Cruz, P. L. Gammel, E. Bucher, and D. J. Bishop, Nature (London) **396**, 348 (1998).
[6] Y. Fasano, J. A. Herbsommer, F. de la Cruz, F. Pardo, P. L. Gammel, E. Bucher, and D. J. Bishop, Phys. Rev. B **60**, R15 074 (1999).
[7] I. V. Grigorieva, L. A. Gurevich, and L. Ya. Vinnikov, Physica C **195**, 327 (1992).
[8] I. V. Grigorieva, J. W. Steeds, and K. Kasaki, Phys. Rev. B **48**, 16 865 (1993).
[9] G. J. Dolan, G. V. Chandrashekhar, T. R. Dinger, C. Feild, and F. Holtzberg, Phys. Rev. Lett. **62**, 827 (1989).
[10] P. L. Gammel *et al.*, Phys. Rev. Lett. **69**, 3808 (1992).
[11] G. Van Tandeloo, D. Broddin, H. W. Zandbergen, and S. Amelinckx, Physica C **167**, 627 (1990).
[12] D. Feinberg and C. Villard, Phys. Rev. Lett. **65**, 919 (1990).
[13] G. Blatter, J. Rhyner, and V. M. Vinokur, Phys. Rev. B **43**, 7826 (1991).
[14] J. A. Herbsommer, J. Luzuriaga, L. Civale, G. Nieva, G. Pasquini, H. Lanza, and P. Levy, Physica C **304**, 112 (1998).
[15] A. V. Silhanek, L. Civale, S. Candia, G. Nieva, G. Pasquini, and H. Lanza, Phys. Rev. B **59**, 13 620 (1999).
[16] A. A. Zhukov, G. K. Perkins, J. B. Thomas, A. D. Caplin, H. Küpfer, and T. Wolff, Phys. Rev. B **56**, 3481 (1997).
[17] C. A. Bolle, P. L. Gammel, D. G. Grier, C. A. Murray, D. J. Bishop, D. B. Mitzi, and A. Kapitulnik, Phys. Rev. Lett. **66**, 112 (1991).
[18] P. L. Gammel, D. J. Bishop, J. P. Rice, and D. M. Ginsberg, Phys. Rev. Lett. **68**, 3343 (1992).
[19] F. de la Cruz, D. Lopez, and G. Nieva, Philos. Mag. B **70**, 773 (1994).
[20] P. L. Gammel, D. J. Bishop, G. J. Dolan, J. R. Kwo, C. A. Murray, L. F. Schneemeyer, and J. V. Waszczak, Phys. Rev. Lett. **59**, 2592 (1987).
[21] G. J. Dolan, F. Holtzberg, C. Feild, and T. R. Dinger, Phys. Rev. Lett. **62**, 2184 (1989).
[22] Z. Hao, J. Clem, M. McElfresh, L. Civale, A. Malozemoff, and F. Holtzberg, Phys. Rev. B **43**, 2844 (1991).
[23] J. Frenkel and T. Kontorowa, Phys. Z. Sowjetunion **13**, 1 (1938).
[24] F. C. Frank and J. H. van der Merwe, Proc. R. Soc. London, Ser. A **198**, 205 (1949).
[25] P. Bak, Rep. Prog. Phys. **45**, 587 (1982).
[26] J. Guimpel, L. Civale, F. de la Cruz, J. Murduck, and I. Schuller, Phys. Rev. B **38**, 2342 (1988).
[27] B. I. Ivlev, N. B. Kopnin, and M. M. Salomaa, Phys. Rev. B **43**, 2896 (1991); V. G. Kogan, N. Nakagawa, and S. L. Thiman, *ibid.* **42**, 2631 (1990); A. I. Buzdin and A. Yu. Simonov, Pis'ma Zh. Éksp. Teor. Fiz. **51**, 191 (1990) [JETP Lett. **51**, 191 (1990)]; A. V. Balatskii, L. I. Burlachkov, and L. P. Gorkov, Zh. Éksp. Teor. Fiz. **90**, 1478 (1986) [Sov. Phys. JETP **63**, 866 (1986)]; A. M. Grishin *et al.*, *ibid.* **97**, 1930 (1990) [**70**, 1089 (1990)].
[28] M. V. Marchevsky, Ph.D. thesis, Leiden University, 1997.
[29] F. Pardo, A. P. Mackenzie, F. de la Cruz, and J. Guimpel, Phys. Rev. B **55**, 14 610 (1997).
[30] S. A. Grigera, E. Morre, E. Osquiguil, C. Balseiro, G. Nieva, and F. de la Cruz, Phys. Rev. Lett. **81**, 2348 (1998).
[31] A. M. Campbell and J. E. Evetts, Adv. Phys. **21**, 199 (1972).
[32] M. W. Coffey and J. R. Clem, Phys. Rev. B **45**, 10 527 (1992).
[33] W. K. Kwok, J. A. Fendrich, V. M. Vinokur, A. E. Koshelev, and G. W. Crabtree, Phys. Rev. Lett. **76**, 4596 (1996).